APPLICATION OF THE SRI CLOUD-TRACKING TECHNIQUE TO RAPID-SCAN GOES OBSERVATIONS

(NASA-CR-159989) APPLICATION OF THE SRI CLOUD-TRACKING TECHNIQUE TO RAPID-SCAN GOES OBSERVATIONS Final Report, 5 Jun. 1978 - 30 Jan. 1980 (SRI International Corp., Menlo Park, Calif.) 34 p HC A03/MF A01 CSCL 05B G3/42

N80-26711

Unclas 27837

Final Report

March 1980

By: Daniel E. Wolf, Senior Research Mathematician
Roy M. Endlich, Senior Research Meteorologist
Atmospheric Science Center

Prepared for:

National Aeronautics and Space Administration
Goddard Space Flight Center
Greenbelt, Maryland 20771

Attn: Dr. A.F. Hasler, Code 911

Contract NAS5-25027

SRI Project 7505

SRI International
333 Ravenswood Avenue
Menlo Park, California 94025
(415) 326-6200
Cable: SRI INTL MPK
TWX: 910-373-1246

Technical Report Documentation Page

1. Report No.	2. Government Accession No.	3. Recipient's Catalog No.

4. Title and Subtitle
APPLICATION OF THE SRI CLOUD-TRACKING TECHNIQUE TO RAPID-SCAN GOES OBSERVATIONS

5. Report Date
March 1980

6. Performing Organization Code

7. Author(s)
Daniel E. Wolf and Roy M. Endlich

8. Performing Organization Report No.
Final Report
SRI Project 7505

9. Performing Organization Name and Address
SRI International
333 Ravenswood Avenue
Menlo Park, California 94025

10. Work Unit No. (TRAIS)

11. Contract or Grant No.
NAS5-25027

12. Sponsoring Agency Name and Address
National Aeronautics and Space Administration
Goddard Space Flight Center
Greenbelt, Maryland 20771
Attn: Dr. A.F. Hasler, Code 911

13. Type of Report and Period Covered
Final Report
5 Jun 78 - 30 Jan 80

14. Sponsoring Agency Code

15. Supplementary Notes

16. Abstract

This investigation improved the SRI automatic cloud tracking system so that it can be applied to multilayer clouds associated with severe storms. The method has been tested using rapid-scan observations of Hurricane Eloise obtained by the GOES satellite on 22 Septebmer 1975. SRI performed cloud tracking using clustering based either on visible or infrared data and tracked the clusters using two different techniques. For data of 4-km and 8-km resolution, the automatic system gave results very comparable in accuracy and coverage to those obtained by NASA analysts using the Atmospheric and Oceanographic Information Processing System (AOIPS). We recommend that the automatic system be included as an option on AOIPS so that more extensive testing and evaluation can be carried out.

17. Key Words	18. Distribution Statement
Automatic cloud tracking Atmospheric and Oceanographic Information Processing System (AOIPS)	

19. Security Classif. (of this report)	20. Security Classif. (of this page)	21. No. of Pages	22. Price
Unclassified	Unclassified	33	

Form DOT F 1700.7 (8-72) Reproduction of completed page authorized

PREFACE

The SRI Automatic Tracking System (SATS) is an objective cloud-tracking technique for automatically computing cloud motion vectors from digital picture data recorded by geosynchronous weather satellites. It includes steps that select potential tracers from each frame, identify the same tracer in successive frames, and convert the displacements into motion vectors. Since the computations are made without intervention by the operator, the system has good potential for coping with large volumes of data for research and operational uses.

In this study, we have significantly improved the automatic system. One major improvement provides better targets for tracking, particularly at cloud edges or in other areas of strong gradients in the data. A second change minimizes the number of spurious vectors computed near area boundaries. A third change allows the MOTION routine to calculate cloud displacements in as many as four separate layers simultaneously. The improvements were tested using data for complicated multilevel cloud motions. The cloud motions took place in the vicinity of the eye of hurricane Eloise as it passed across the Gulf of Mexico on September 22, 1975. On this data, NASA Goddard personnel obtained rapid-scan observations separated by 10 minutes or less. These images show that just to the northwest of the eye, there was high-speed outflow at the cirrus level. The cirrus shield had a sharp north-south edge. To the west of the cirrus edge, low clouds were moving in the opposite direction. Using infrared data for target selection, the automatic system was able to follow these motions. To the south of the eye, clouds were mainly cumuloform, and the automatic tracking following the motions using either visible or infrared data in the target selection (grouping) process. The method was successful also in tracking motions in other nearby sectors of the hurricane.

We have evaluated the automatic motions qualitatively by comparing them to the flow shown in a rapid-scan movie of Eloise made available to us by NASA-Goddard personnel. We have also compared the computer-determined motions qualitatively to those measured by NASA analysts and there is good overall agreement. For data with 4-km and 8-km resolution, the automatic system obtained a coverage of motions that was very similar to that obtained by the human analysts using data of comparable resolution.

We have introduced a cross-correlation computation as an option in SATS and have compared cloud displacements computed by the MOTION program and by the cross-correlation technique. The cross-correlation computation uses the visible or infrared targets selected automatically, and

finds their point of best fit by using a search routine. The accuracy of the results is similar to that of the MOTION routine; however, cross correlation has the advantage that it gives a denser coverage of cloud motion vectors.

We believe that the cloud motion vectors computed using the SRI automatic system are now competitive in accuracy and coverage with motion fields determined by human analysts working within reasonable time limits. We recommend that the automatic system be included as an option on AOIPS so that larger scale testing and evaluation can be carried out.

CONTENTS

ILLUSTRATIONS

TABLES

I INTRODUCTION

With the recent deployment of four or more geosynchronous weather satellites around the globe, a very large amount of data concerning the earth's cloud cover is acquired each day. The data are more than adequate for achieving the long-term goal of determining cloud motions in real time over much of the globe, but the present processing methods are far too slow. This report describes our most recent work toward improving the automatic cloud tracking methodology that has been under development for several years (Endlich et al., 1971; Wolf et al., 1977). We believe that an automatic method of this sort combined with recent advances in computers and display systems can significantly enhance the usefulness of geosynchronous satellite observations for research, and probably also for operations with consequent economic benefits.

We have made significant improvements to the automatic system. The improvements are demonstrated in tests with a small sample of data for complex cloud motions in the vicinity of the eye of hurricane Eloise. Special rapid-scan data were obtained for this storm as it traveled through the Gulf of Mexico on September 22, 1975. For these data, cloud motion measurements were made by meteorological analysts using the Atmospheric and Oceanographic Information Processing System (AOIPS) described by Billingsley (1976). These measurements have been described by Rodgers et al. (1979) and we have used them in evaluating the automatic computations. As the SRI system has been discussed in considerable detail by Wolf et al. (1977), in this report we give only those details needed to describe the recent changes to it. Also, to compare our computations with the well-known cross-correlation method (see for example Leese et al., 1971; Bauer, 1976; Hasler et al., 1976), we have imbedded a cross-correlation computation in our methodology. This allows us to track cloud targets in two different ways--i.e., using the MOTION program or using cross correlation.

II CHANGES MADE TO THE AUTOMATIC METHOD

The major steps in the automatic method are shown in Figure 1. In the present study, substantial changes have been made in Steps 4 and 6. To separate trackable cloud groups from background (Step 4) we must first calculate a smoothed picture. This computation is done by the TRIANG routine, which uses triangular weights for elements within a specified window (usually taken as 21 by 21 elements) around each pixel. The previous version, based on logic similar to that used in fast Fourier transforms, allowed the window to "wrap around" at the end of a line or column. This distorted the smoothed picture within a distance of one-half the window width from the edges. The new version does not allow wraparound, and gives a smoothed picture that is reliable to within two or three elements from an edge. This change aids substantially in reducing the number of spurious motion vectors computed near edges.

The subroutine DEVIATE in Step 4 computes the difference between the brightness (or infrared value) at each point and the smoothed brightness at the same point. Then it selects 50 percent of the points that are brighter than the smoothed picture and organizes them into "touching groups." A "touching group" is defined as all points that touch at least one other member of the group, with touching defined as being adjacent to the left, right, up, down, or along diagonals. This procedure usually gives some groups that are too large and irregular to serve as good tracers. The DELETE algorithm eliminates extraneous points from large groups, but for small groups (less than 10 points), all points are retained. For the larger groups, the proportion of points eliminated rises to 50 percent for groups having 50 points or more. The DELETE algorithm is normally repeated three times.

We have found that the logic for eliminating points from groups is critically important in giving good results. In the old version of DELETE, a cumulative brightness distribution was made for each group. Then a threshold was set at the particular brightness value such that the desired number of points in the group was retained. This dropped the dimmest members of the group, and often separated the group into two or more parts (created two smaller groups), as desired. However, it also had the undesirable property that it tended to discard points along cloud edges. The new version of DELETE operates on deviations in brightness rather than on brightness itself. Since deviations in brightness tend to be large along cloud edges (such as the edges of cirrus bands), the improved algorithm retains relatively bright edge targets of the sort tracked by human analysts. This change has added significantly to the accuracy of the methodology.

To demonstrate this change, we applied DELETE to infrared data for hurricane Eloise. Figures 2 and 3 show visible and infrared data for an

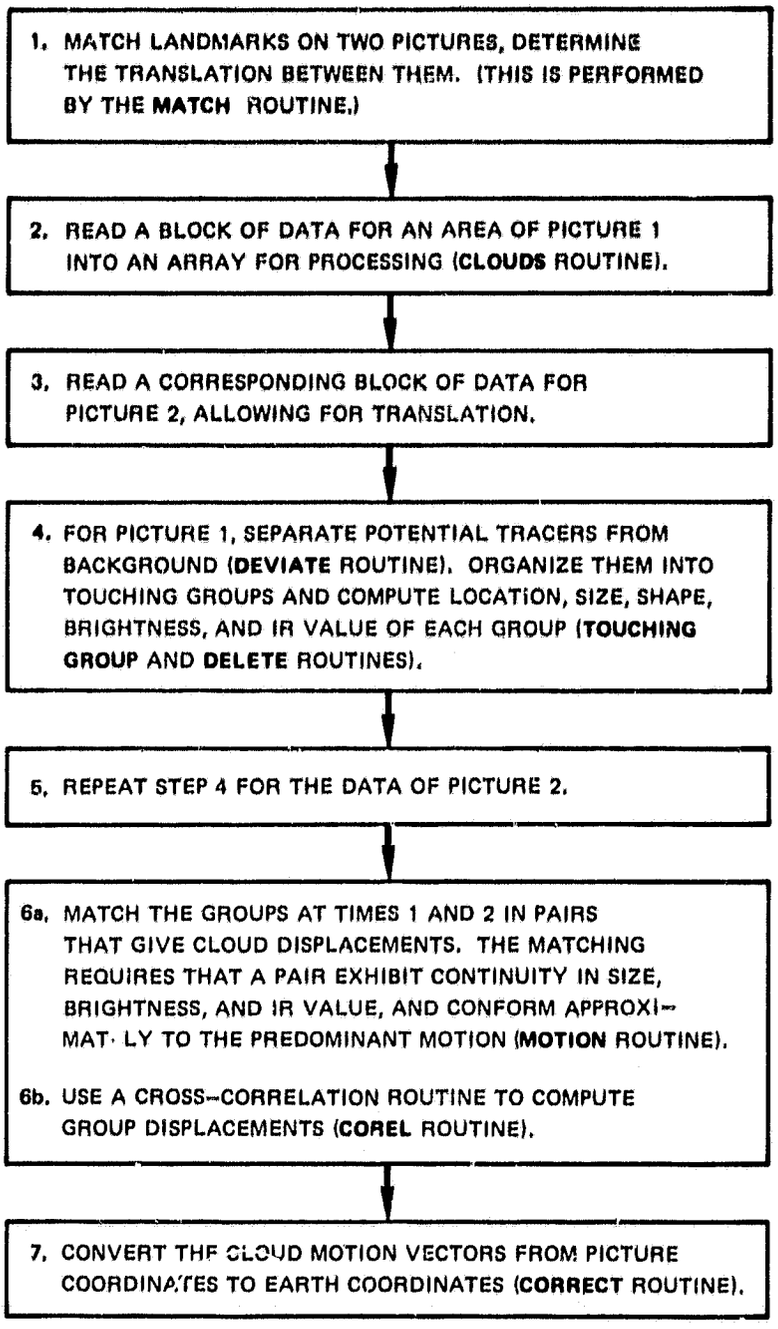

FIGURE 1 BLOCK DIAGRAM OF THE AUTOMATIC CLOUD TRACKING SYSTEM

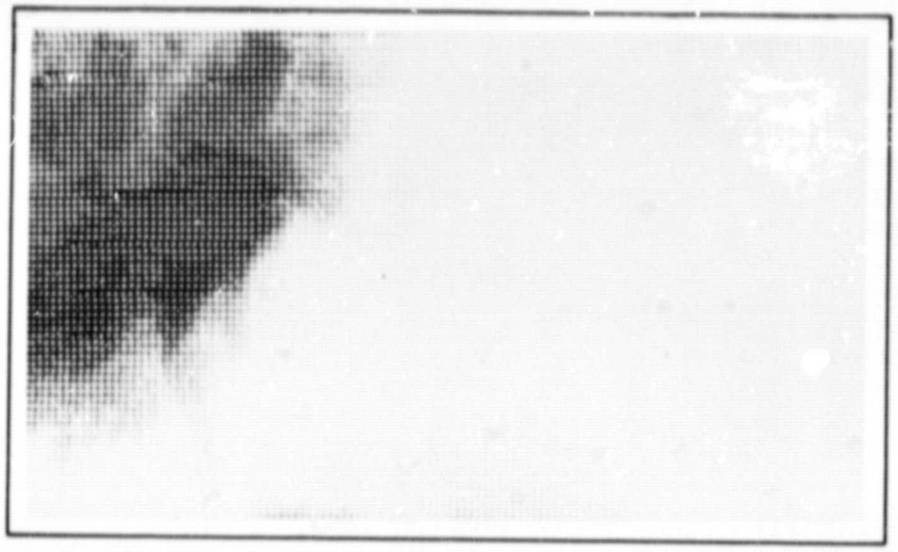

FIGURE 2 VISIBLE IMAGE OF THE NORTHWEST SECTOR OF HURRICANE ELOISE AT 1932 GMT, SEPTEMBER 22, 1975
The area covered is 560 by 1000 km. The eye is in the southeast corner. The data array consists of 70 by 120 elements of approximately 8-km resolution.

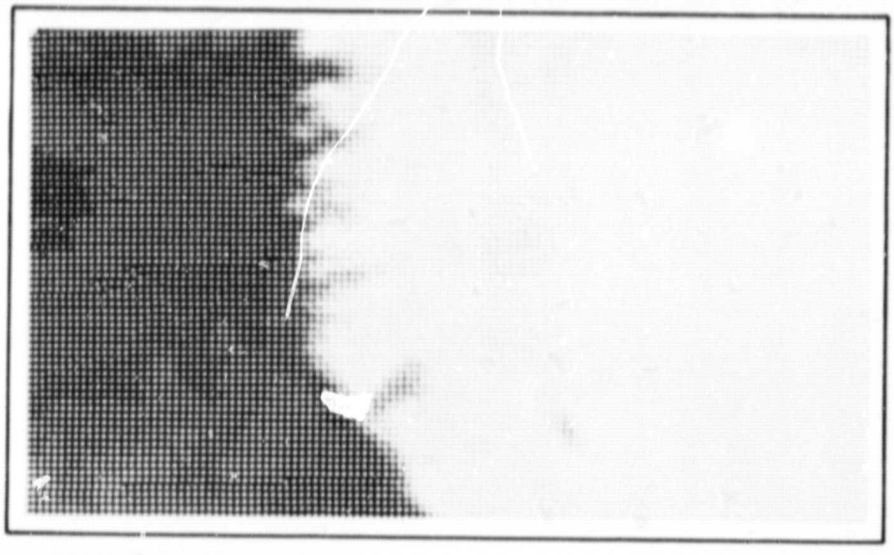

FIGURE 3 INFRARED IMAGE FOR THE SAME TIME AND AREA AS FIGURE 2

area approximately 560 km north-south by 1000 km east-west with the eye (rather indistinct) in the southeast corner. Figures 4, 5, and 6 show the groups that remain after successive applications of DELETE. In Figure 6, the groups represent the cirrus along the north-south edge of the cirrus shield and other locally cold clouds. In the next step (Figure 7), groups that are very small (having less than two members) are discarded. Also, to avoid edge contamination in the motions, we eliminated groups that touch an edge.

If the grouping is done using visible rather than infrared data, the results are analogous to those shown above. However, due to differences between Figures 2 and 3, the visible groups are generally not the same as the infrared groups.

As described by Wolf et al. (1977), the MOTION routine pairs groups on successive pictures. This is done by matching a group at time 1 with the best likeness of itself (in terms of size, brightness, and shape) at time 2, and also requiring that the resulting motion vector conform approximately to the average motion within the area being considered. This rationale is intended to follow the tracking concepts used by human analysts. The recent changes made in Step 6 of Figure 1 enable the MOTION routine to compute cloud motions simultaneously in four separate layers. The cloud groups are divided into four categories using the mean infrared value for each group based on threshold values of less than 101, 101 to 140, 141 to 180, and greater than 180, respectively. These categories tend to separate the clouds into low, middle, high, and deep convective types. The rationale for this very simple scheme is that the touching groups represent locally broken or overcast clouds; therefore the average infrared values are closely related to the cloud-top temperatures.

With the groups separated into four categories, the MOTION program computes an average motion for each layer. These averages normally differ from each other. In the iterations within MOTION, the averages are used to determine whether each candidate motion conforms sufficiently well to the associated average for that layer to be a member of the family. The height category is printed beside each vector in subsequent figures.

Figure 8 shows the MOTIONS computed for a pair of rapid-scan pictures separated in time by approximately 10 minutes. The grouping was done using infrared data, and the visible data were used as an additional tag in the MOTION computations (see Wolf et al., 1977). The low clouds are traveling generally southward with an average speed of 13 m s^{-1}, and the high clouds (layers 3 and 4) are moving at an average speed of 18 m s^{-1}, generally toward the north. The maximum computed speed is 42 m s^{-1} (82 knots) for the northernmost vector in layer 3, which is for a target lying in the edge of the cirrus clouds. Figure 9 shows motions computed between a rapid-scan pair approximately one-half hour after the first pair. The results are quite similar. Figure 10 shows motions computed between two slightly later pictures separated by 30 minutes instead of 10 minutes. Fewer vectors are computed for the longer time interval

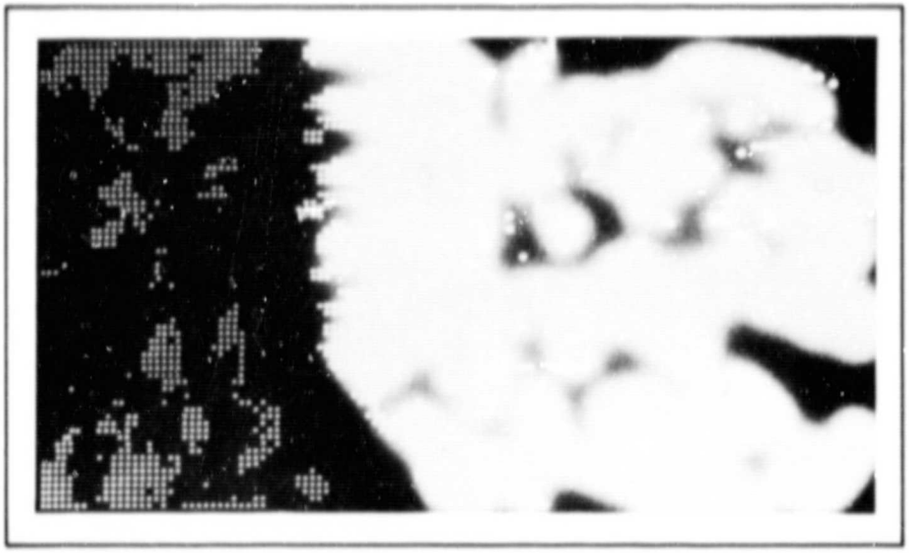

FIGURE 4 IMAGE OF THE POSITIVE INFRARED DEVIATIONS (LOCAL VALUES MINUS THE SMOOTHED BACKGROUND)

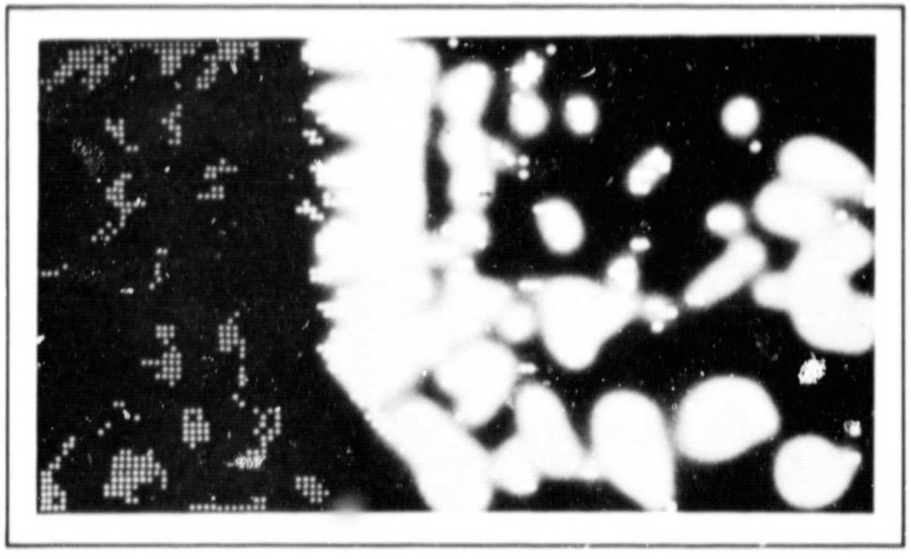

FIGURE 5 CLOUD TARGETS (TOUCHING GROUPS) BASED ON INFRARED DATA AFTER ONE ITERATION OF THE DELETE SUBROUTINE

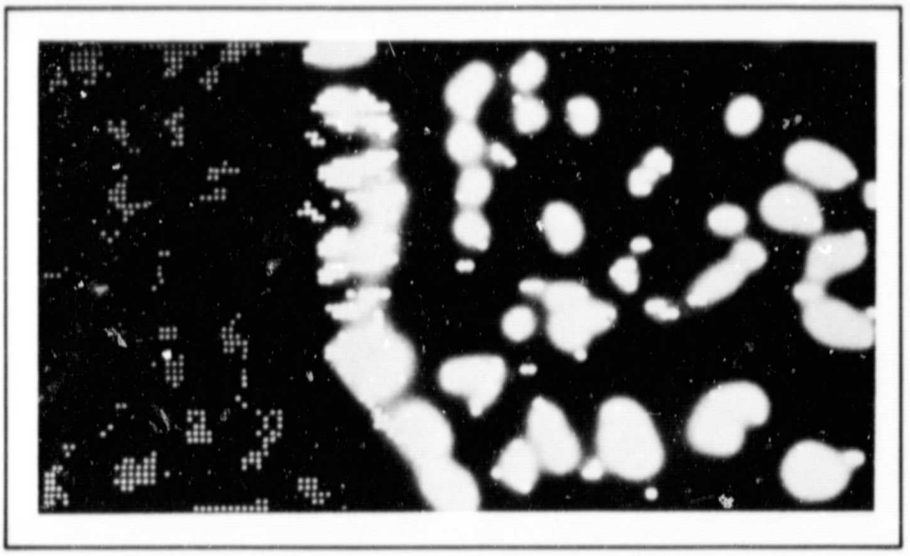

FIGURE 6 CLOUD TARGETS AFTER TWO ITERATIONS

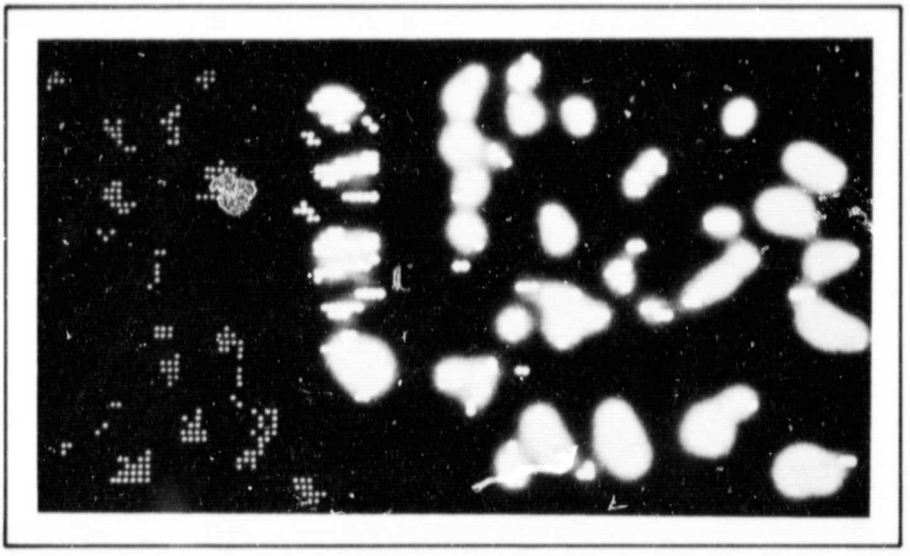

FIGURE 7 CLOUD TARGETS AFTER THREE ITERATIONS AND WITH GROUPS THAT ABUT EDGES DELETED

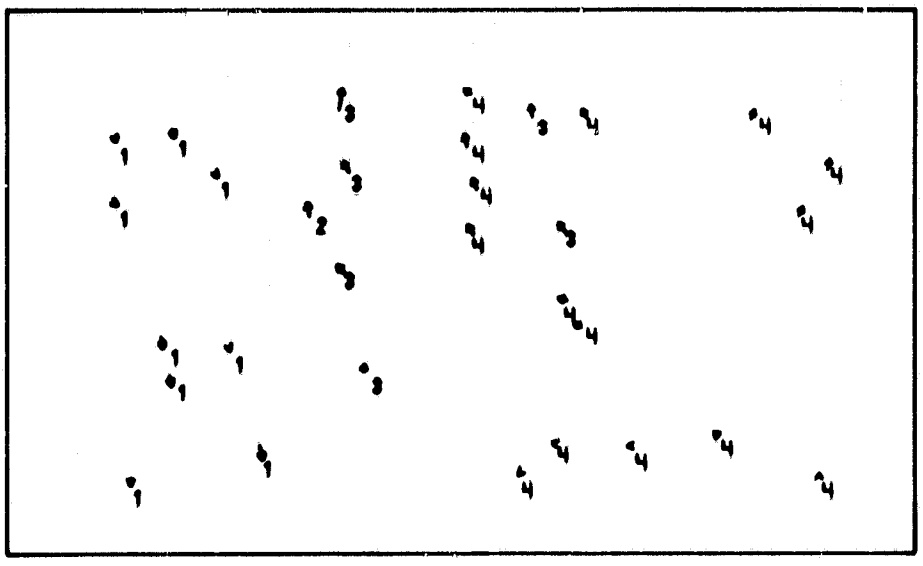

FIGURE 8 CLOUD MOTION VECTORS COMPUTED FROM THE GROUPS OF FIGURE 7 AND THE NEXT RAPID-SCAN IMAGE APPROXIMATELY 10 MINUTES LATER, SHOWING CIRRUS OUTFLOW AND OPPOSITE LOW-LEVEL FLOW
The numbers 1 to 4 designate cloud heights.

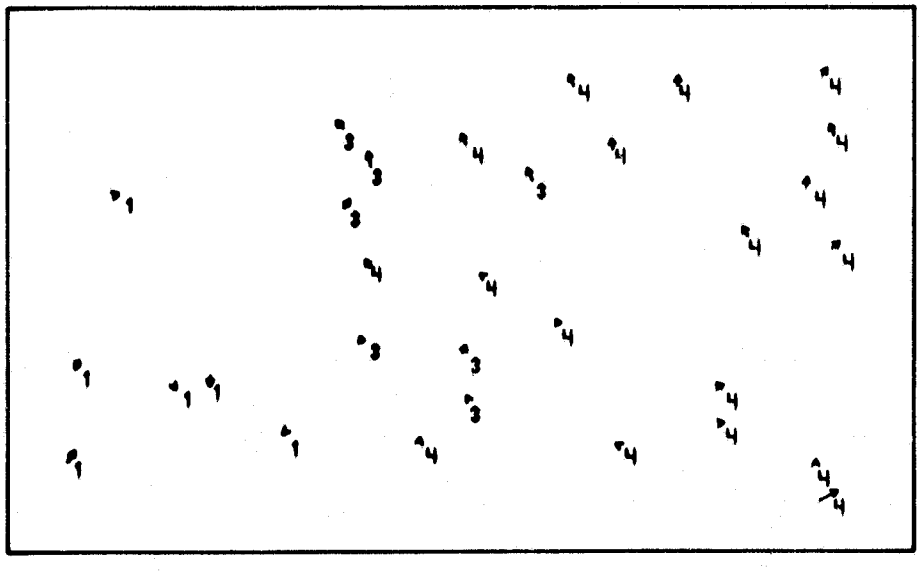

FIGURE 9 MOTION VECTORS APPROXIMATELY ONE-HALF HOUR AFTER FIGURE 8

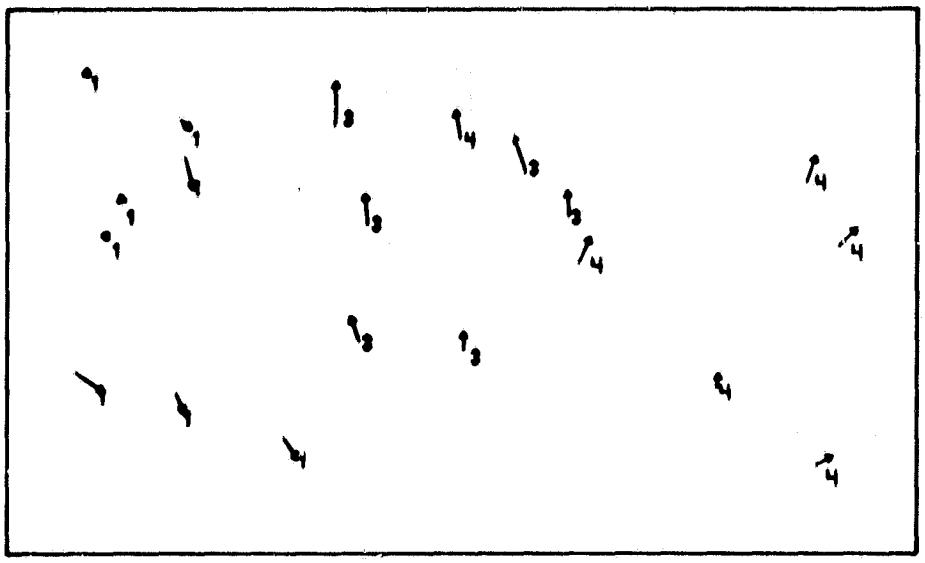

FIGURE 10 MOTION VECTORS COMPUTED USING INFRARED IMAGES SEPARATED BY 30 MINUTES

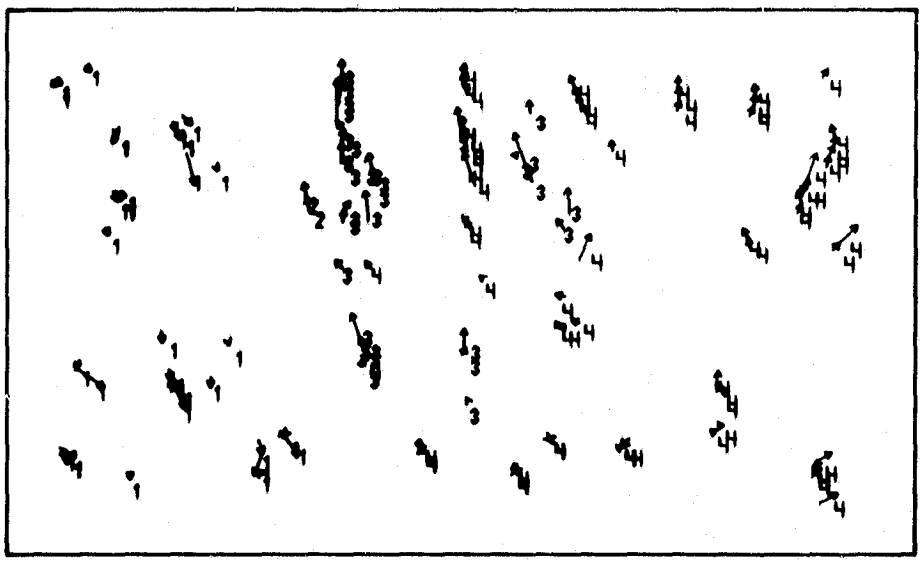

FIGURE 11 THE SERIES OF CLOUD MOTION VECTORS COMPUTED USING SIX SUCCESSIVE RAPID-SCAN IMAGES EXCEPT FOR THE LAST PAIR, WHICH HAS THE NORMAL 30-MINUTE INTERVAL

because local dynamic changes in the clouds prevent the MOTION program from making reliable matches for many groups. Of course the motions are approximately three times larger than in Figures 8 and 9. Figure 11 summarizes the cloud motions computed using the sequence of six tapes of 8-km resolution data including the 30-minute time difference. It can be seen that the motions have a consistent pattern; however, there are a few vectors, probably erroneous, that are at odds with their neighbors.

Figure 12 shows the motions computed using grouping based on visible data for the same time as in Figure 8. Since the visible data (Figure 2) do not have as much contrast between low and high clouds as the infrared data contain, the computed field of visible motions in the center of the picture is rather confused and may be unreliable. For this sequence, better results were obtained using infrared grouping.

These figures illustrate the principal improvements that have been made to the SATS programs during the present contract. These improvements are crucial in obtaining accurate results in cases of complicated and rapidly changing clouds. For simpler motions, such as those associated with the translation of a single layer of clouds, the previous version of SATS performed satisfactorily. We are confident that the improvements are also beneficial, though to a lesser extent, for such cases.

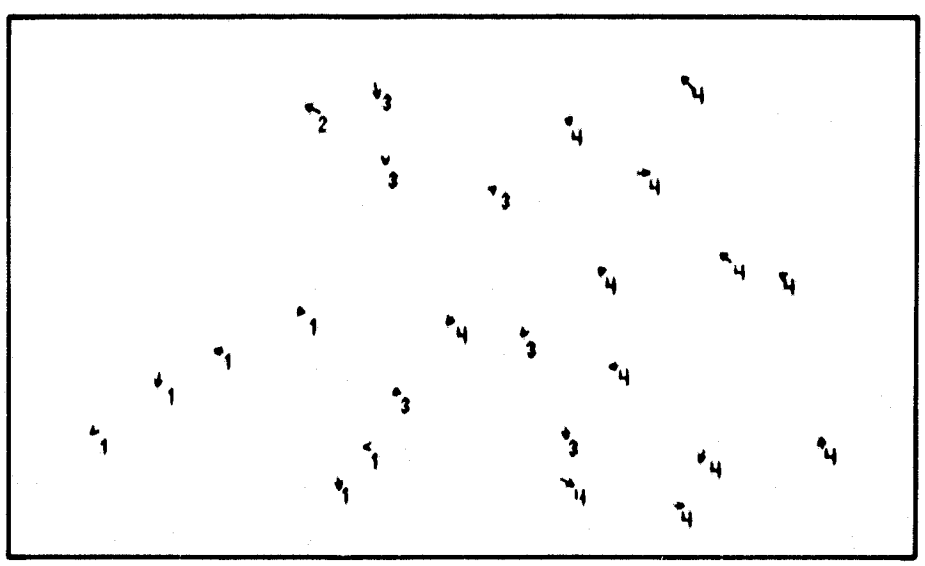

FIGURE 12 CLOUD MOTIONS COMPUTED USING VISIBLE GROUPING OF 8-km RESOLUTION DATA FOR THE SAME PICTURE PAIR AS IN FIGURE 8

III INTRODUCTION OF A CROSS-CORRELATION COMPUTATION

The most common method for making objective computations of cloud displacements uses the cross-correlation method described by Leese (1971). This method has been implemented for interactive use on McIDAS (Smith, 1975) and on AOIPS (Hasler et al., 1976). To learn whether the MOTION program gives the same results as would be obtained by applying a cross-correlation computation to the same area of a picture, we have introduced a correlation computation as an option in SATS. The computation uses the groups produced by the DEVIATE and DELETE routines. These groups are targets that are analogous to the cloud features selected by human analysts. In our usage, the target is taken as a 7 by 7 pixel area centered on the position of a group. The correlations are not computed at every point within a large area of picture 2 as is usually done. Instead, a search routine is used. At the start of a picture sequence, the search on picture 2 begins at the original location of the array on picture 1. Correlations of picture 1 with picture 2 are computed with the 7 by 7 array centered on the same point and the four neighbors (to the right, left, up and down). The center of the search goes to the point of highest correlation. Correlation computations are made again, and the search continues until it cannot find a higher correlation at a neighboring point. Then correlations are computed at all points within a 3 by 3 (or 5 by 5) area around the peak value. From these values, the point of highest correlation is found by fitting a second-degree polynomial to the nearby correlation coefficients.

After computations are made for the first pair of pictures in a series, the average motion in each cloud layer is computed. This motion is used as a first guess in the search on the next pair of images; this improves the accuracy of the results. The correlation computation has an option for using visible data, infrared data, or both. In the latter case, the data are simply combined since their average values and ranges are approximately the same. This search type of correlation procedure follows that used in landmark matching by Hall et al. (1972). The computations are not made by a fast Fourier transform, but are economical because the search procedure restricts the number of positions that must be examined. In subsequent figures showing vectors determined by cross correlation, a result is given for each target except at edges of the areas. We have not used the magnitude of the correlation coefficient or other information in order to edit the motions.

Figure 13 shows the motion vectors computed using the correlation routine for the same groups of visible data that were tracked by the MOTION routine in Figure 12. There are approximately twice as many vectors as in Figure 12 because every potential target has been used,

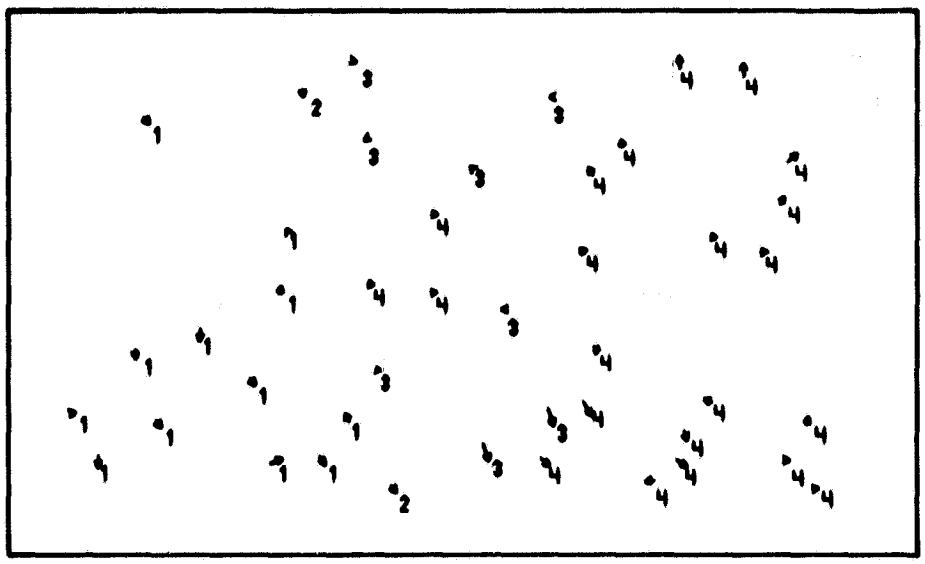

FIGURE 13 CLOUD MOTIONS COMPUTED BY CROSS CORRELATION FOR THE SAME GROUPS OF VISIBLE DATA USED IN FIGURE 12

whereas the MOTION program eliminates a substantial proportion of targets (those that do not give acceptable motions). The pattern of motions appears to be reasonably satisfactory.

IV FURTHER RESULTS OF COMPUTATIONS

To investigate the use of higher resolution data, we made computations for an area that comprises the left central part of Figure 3 using 4-km-resolution data and infrared grouping. As shown in Figure 14, the results appear to be quite satisfactory in representing both the high-level and low-level clouds. For these vectors the average speeds are 11 m s^{-1} in layer 1, 18 m s^{-1} in layer 3, and 15 m s^{-1} in layer 4. There are 24 vectors in this area compared to 17 obtained using the coarser resolution data (Figure 8). Only about 8 high-level vectors were obtained within the region of Figure 14 by Rodgers et al. (1979). However, if the resolution were increased further (e.g., from 4 km to 2 km), the automatic system would probably not be able to cope with the motions because there is a limitation in the initial search by MOTION--namely that the displacement must be less than 6 pixel units in the time interval between the pictures used.

The cloud motions computed using the correlation technique for the same infrared groups used in Figure 14 are shown in Figure 15. The data coverage is good, but the accuracy is rather marginal. In the second picture pair, the average layer values from the first pair are used as the initial guess. The results for the MOTION routine are shown in Figure 16, and for the COREL routine in Figure 17. The latter is considerably improved compared to Figure 15. Similarly, Figures 18 and 19 show the computations for the third picture pair.

Figure 20 shows the cloud motion vectors computed for the series of six images, including a 30-minute separation of the last pair, using 4-km targets followed by the MOTION program. The results are generally consistent and accurate. Numerous targets are tracked over several frames. The comparable vectors computed by cross correlation are shown in Figure 21. Again the results are good, both in accuracy and coverage.

Toward the southern periphery of Eloise the cloud patterns are different than to the north of the eye, being mainly cumuloform but also including some high clouds. Figure 22 shows the 4-km visible image for this area, and Figure 23 shows the infrared data. Figure 24 shows the motion vectors for the first pair of pictures (separated by approximately 10 minutes) based on automatic grouping of the visible data. There is a predominant strong motion of low clouds from the northwest. The average speed of the 18 low-cloud (layer 1) vectors is 18 m s^{-1}. The comparable motions computed by cross correlation are shown in Figure 25. The pattern of low cloud motions is rather confused. For the next pair of pictures, the layer averages of the motions from the previous picture pair were used as a first guess by both the MOTION and COREL routines. The resulting motion fields are shown in Figures 26 and 27. The use of a first

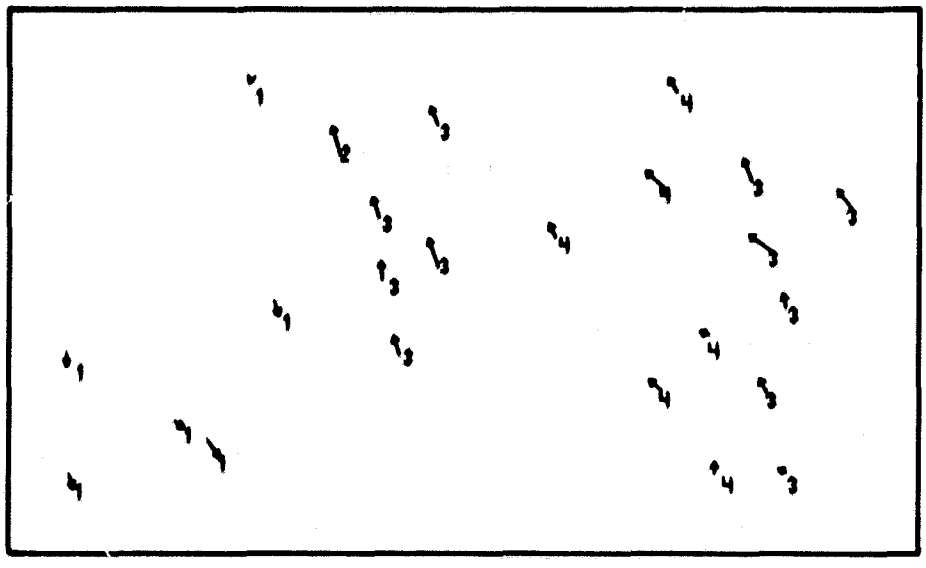

FIGURE 14 CLOUD MOTIONS COMPUTED FOR THE LEFT CENTRAL PORTION OF FIGURE 2 (INCLUDING THE EDGE OF THE CIRRUS SHEET) USING 4-km INFRARED DATA
Compare to the coarser resolution of Figure 8.

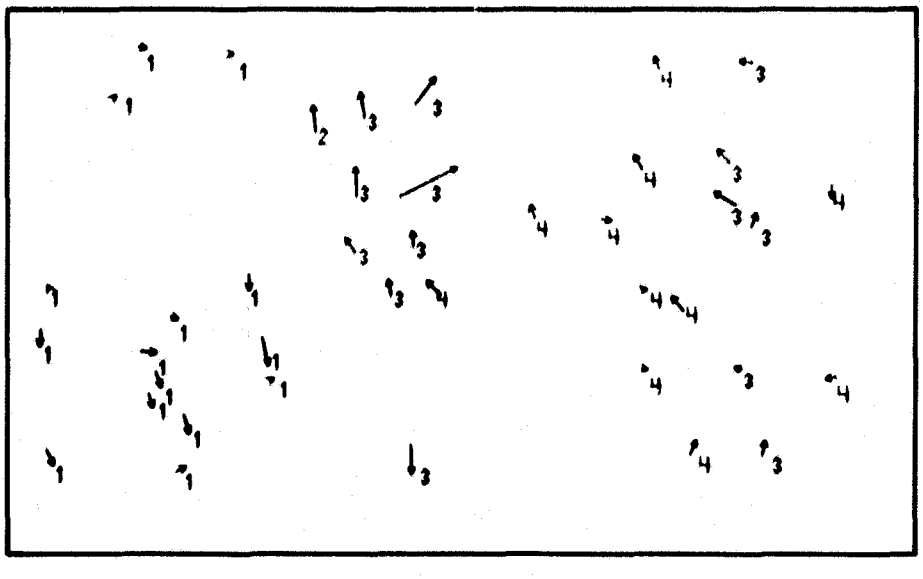

FIGURE 15 CLOUD MOTIONS COMPUTED BY CROSS CORRELATION FOR THE SAME INFRARED GROUPS USED IN FIGURE 14

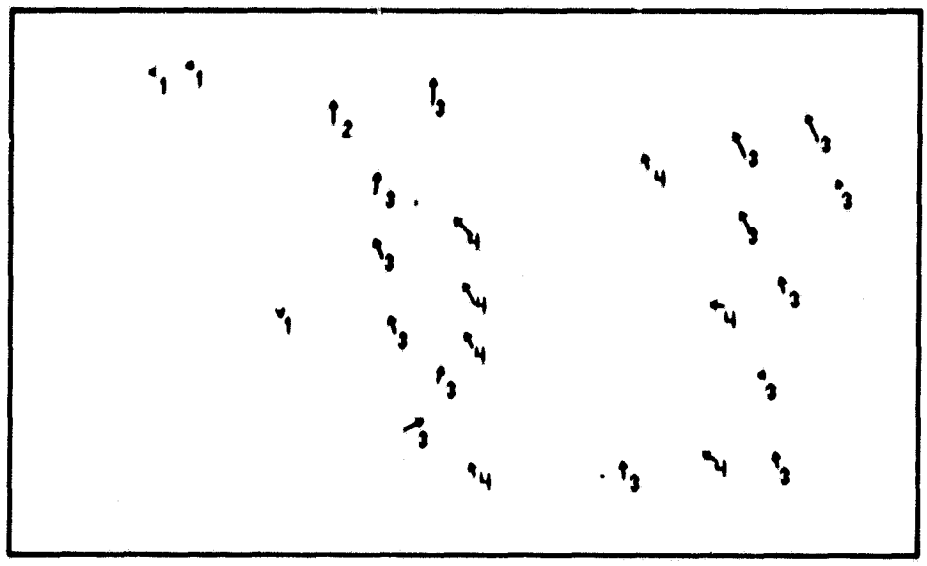

FIGURE 16 CLOUD MOTIONS FOR THE SECOND PICTURE PAIR COMPUTED USING THE MOTION ROUTINE

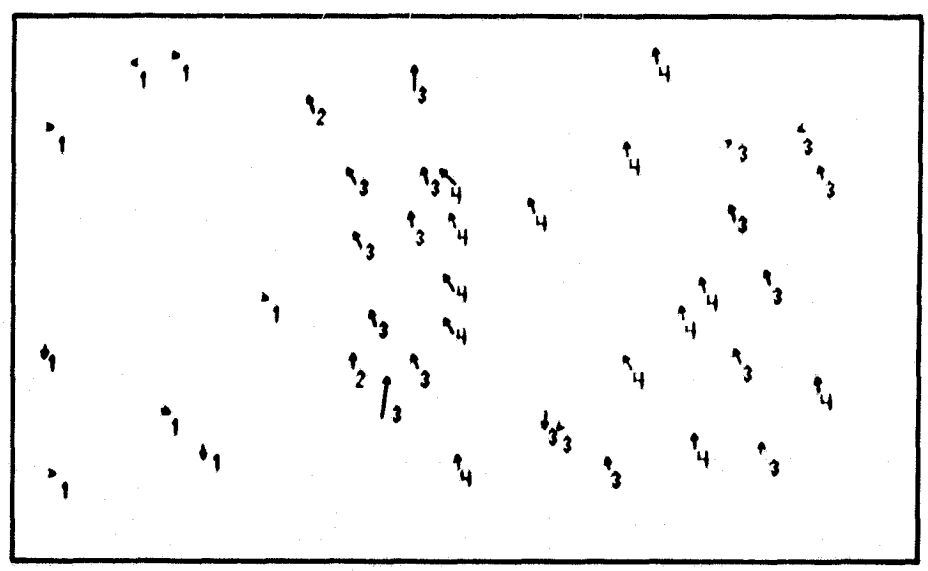

FIGURE 17 CLOUD MOTIONS COMPUTED BY CROSS CORRELATION FOR THE SAME INFRARED GROUPS USED IN FIGURE 16

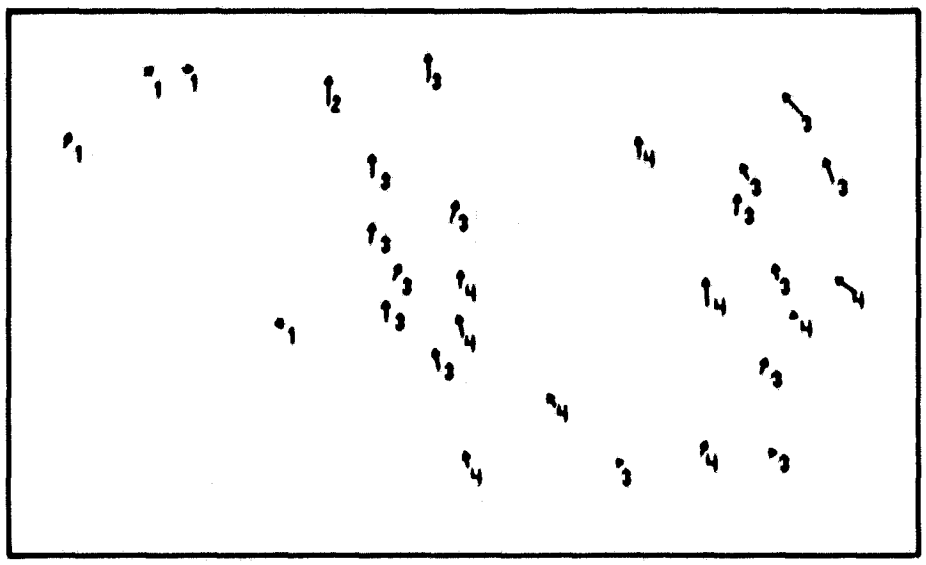

FIGURE 18 CLOUD MOTIONS FOR THE THIRD PICTURE PAIR COMPUTED USING THE MOTION ROUTINE

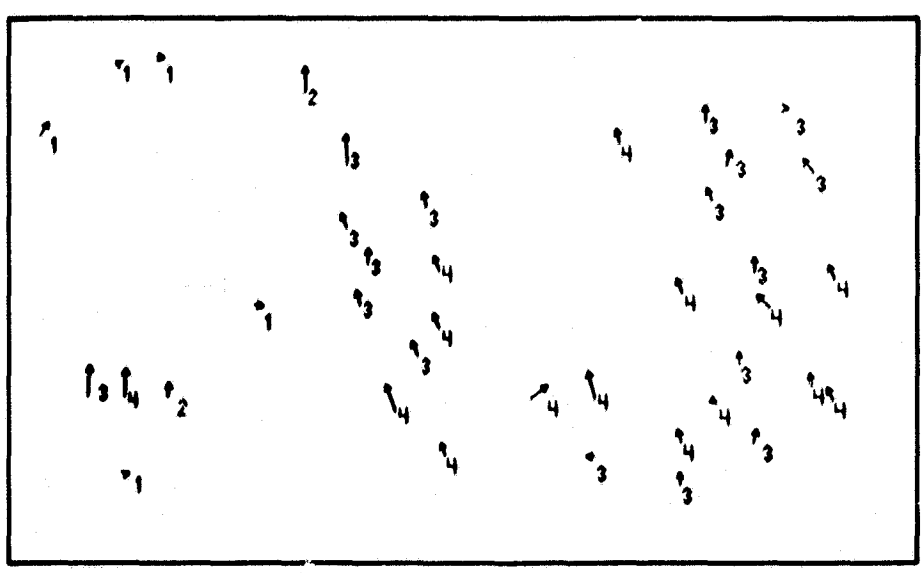

FIGURE 19 CLOUD MOTIONS COMPUTED BY CROSS CORRELATION FOR THE SAME INFRARED GROUPS USED IN FIGURE 18

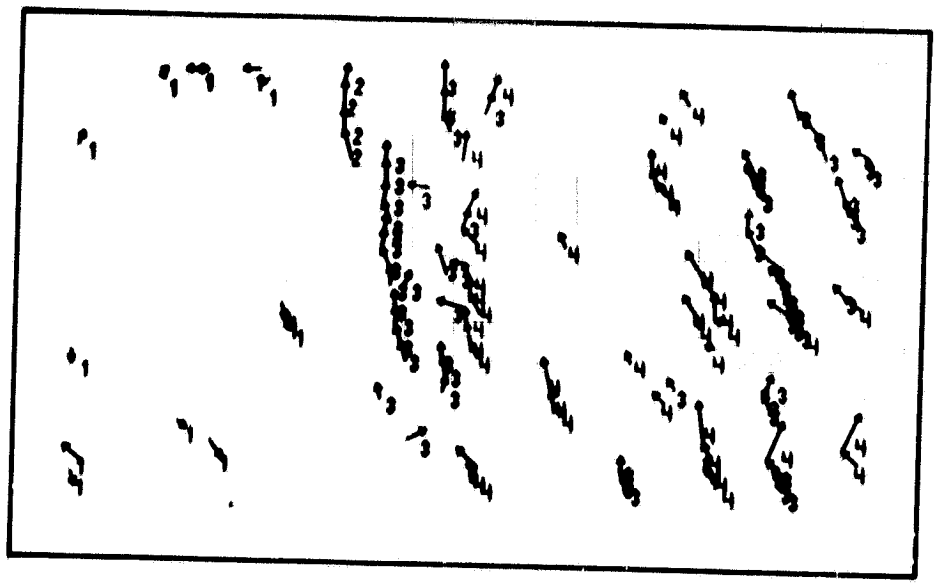

FIGURE 20 CLOUD MOTIONS FOR THE SERIES OF SIX IMAGES OF 4-km INFRARED DATA FOR THE LEFT CENTRAL PORTION OF FIGURE 2, COMPUTED USING THE MOTION ROUTINE

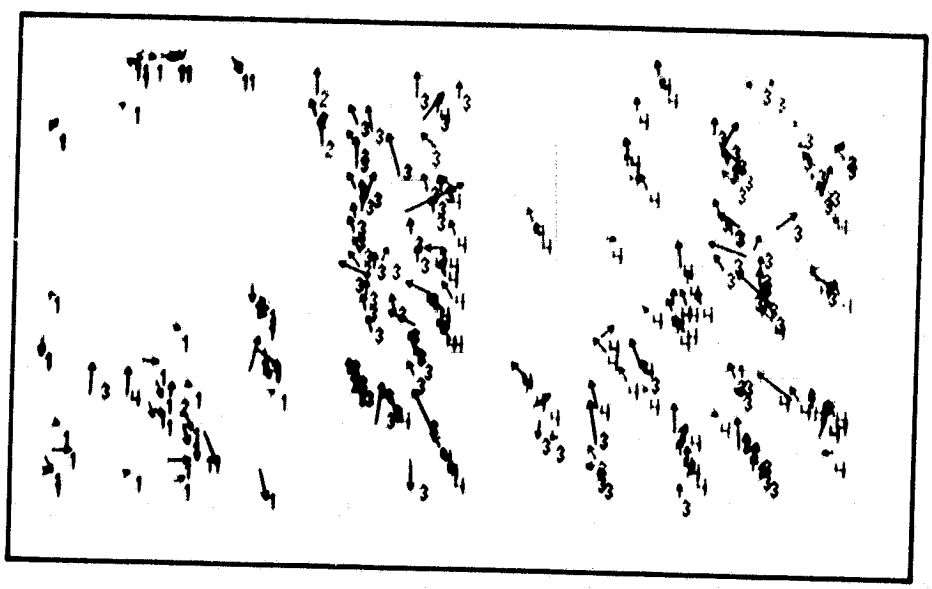

FIGURE 21 CLOUD MOTIONS COMPUTED BY CROSS CORRELATION FOR THE SAME GROUPS USED IN FIGURE 20

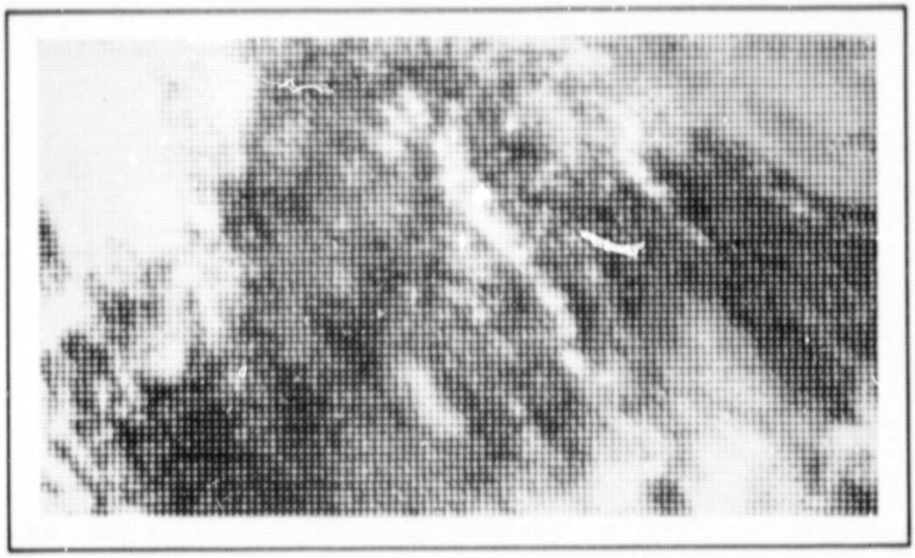

FIGURE 22 VISIBLE IMAGE USING 4-km DATA FOR AN AREA 280 by 480-km TO THE SOUTHWEST OF THE EYE OF ELOISE

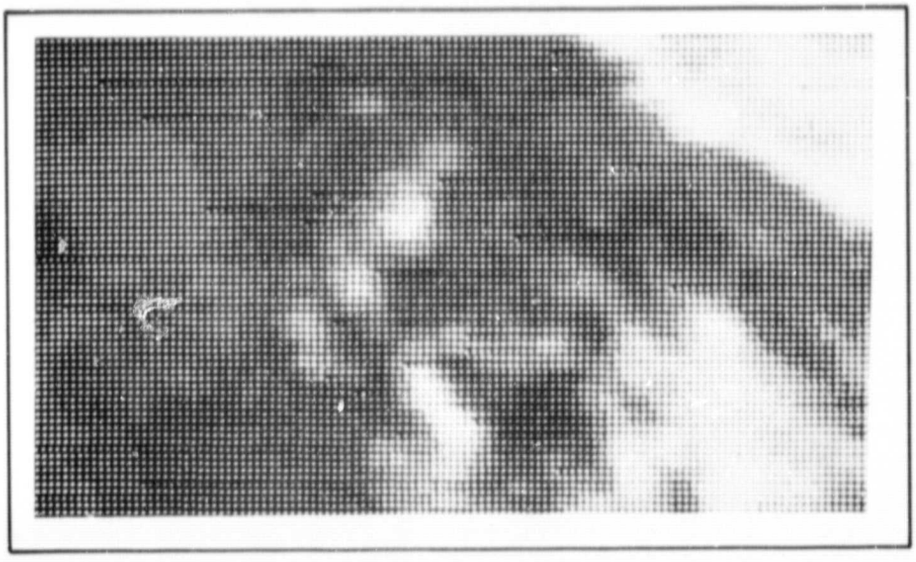

FIGURE 23 IMAGE OF 4-km INFRARED DATA CORRESPONDING TO FIGURE 22

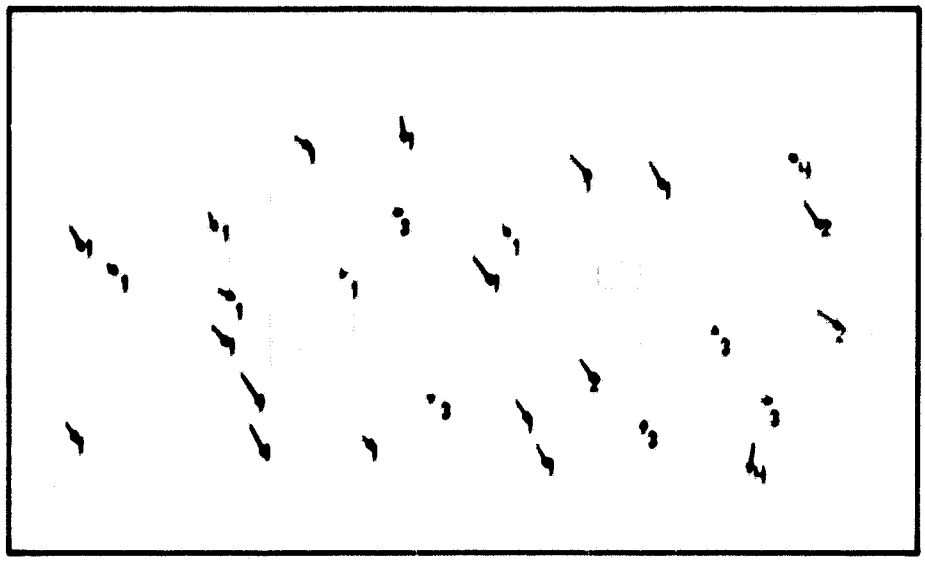

FIGURE 24 CLOUD MOTIONS COMPUTED BY THE MOTION ROUTINE USING VISIBLE TARGETS FOR THE FIRST PICTURE PAIR FOR THE AREA OF FIGURE 22

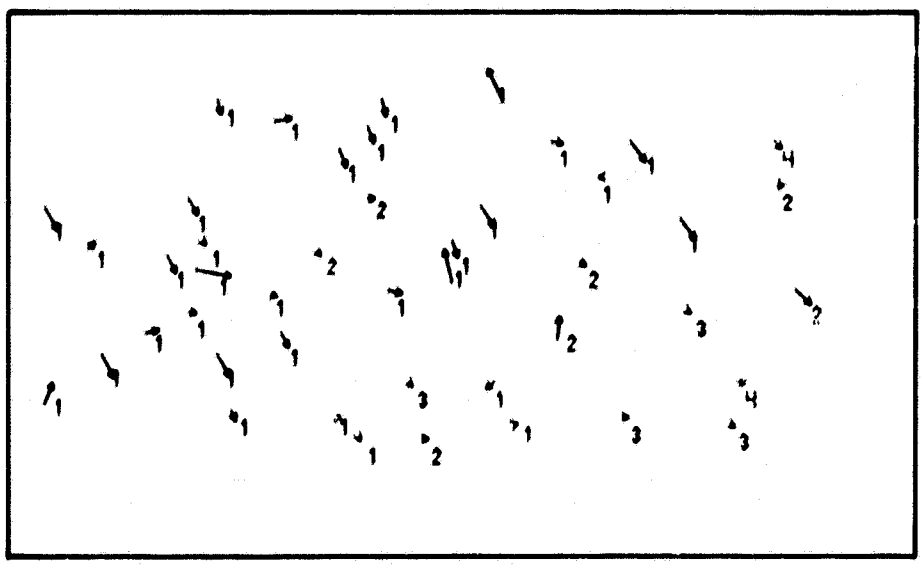

FIGURE 25 CLOUD MOTIONS COMPUTED BY CROSS CORRELATION FOR THE SAME GROUPS USED IN FIGURE 23

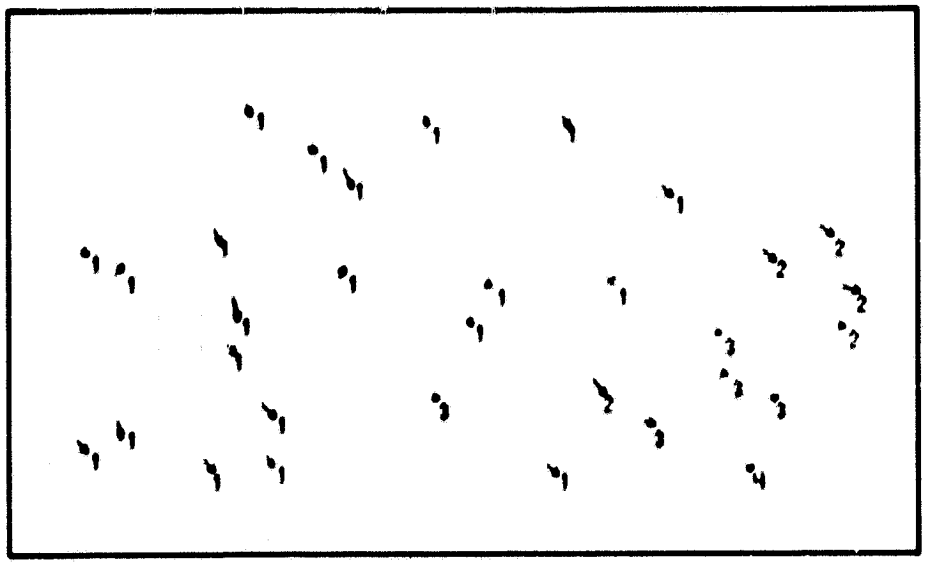

FIGURE 26 CLOUD MOTIONS COMPUTED USING VISIBLE TARGETS FOR THE SECOND PICTURE PAIR

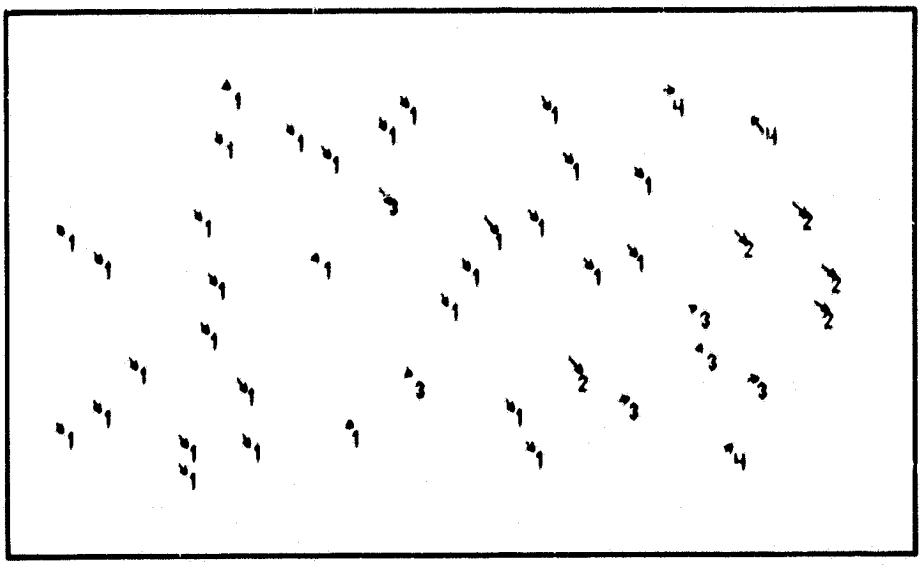

FIGURE 27 CLOUD MOTIONS COMPUTED BY CROSS CORRELATION FOR THE SAME GROUPS USED IN FIGURE 26

guess improves the results. Figure 27 has the better coverage of vectors. The results for the third pair of pictures are shown in Figures 28 and 29. Figure 30 shows the cloud motions for the five picture pairs of the series computed by the MOTION routine using visible data. The patterns are quite acceptable. Figure 31 shows computations for the same targets computed by the COREL routine. The spurious vectors were computed mainly for the first picture pair. The data coverage is more dense than in Figure 30. Many targets can be identified in Figures 30 and 31 as having been tracked quite similarly by the MOTION and COREL routines. The vectors computed by the MOTION routine using infrared targets are shown in Figure 32. There are fewer low-cloud vectors than in Figures 30 and 31 and more high-cloud vectors. These data, as well as others for cases of multilayer clouds, indicate that to obtain complete motion fields in all layers, it may be best to make tracking computations using both infrared and visible data, if available.

Judging the accuracy of these computed motions is difficult--as is almost always true for cloud motions in severe weather outside the radiosonde network. There are, however, approximate methods that may be used in this case. The first method uses a movie of Eloise prepared by William Shenk of NASA Goddard. By viewing this movie repeatedly or by using a TV display system like AOIPS or the SRI cloud console (Serebreny et al., 1970), one can study any sector and compare the automatically computed motions qualitatively to one's impression. We have used both the movie and the console and feel that the results shown earlier are generally accurate. The second method is to compare our computations to cloud motions determined by Rodgers et al. (1979) for approximately the same period of the history of Eloise. Their computations emphasized visible data with 1-km and 2-km resolution and tracking by skilled analysts. The sequence of rapid-scan images that they used began at 1842 GMT, approximately 45 minutes before the beginning of our sequence. Nevertheless, our results are in good qualitative agreement with theirs.

For example, in Figure 8 we computed a maximum speed of a cirrus target of 42 m s^{-1} (82 knots). In this same area, Rodgers et al. (1979) show speeds from 75 to 85 knots (see their Figure 6). In Figures 25 through 28, the average speed of the low clouds computed with the MOTION routine is 11 m s^{-1} (21 knots), and with the COREL routine is 10 m s^{-1} (19 knots). In this same part of Eloise, Rodgers et al. (1979, Figures 1 and 2) show somewhat higher speeds (between 20 and 50 knots). In Figure 32 we show a slow drift of high clouds toward the northeast, and Rodgers et al. show similar values in their Figure 5. A detailed quantitative comparison could best be made by putting both sets of vectors into AOIPS and viewing them against the animated cloud sequence. This was beyond the scope of this study.

In spite of these limitations in validating the automatically computed cloud motions, we believe that they appear qualitatively very satisfactory, and competitive in accuracy and spatial coverage to those obtained by Rodgers et al. (1979).

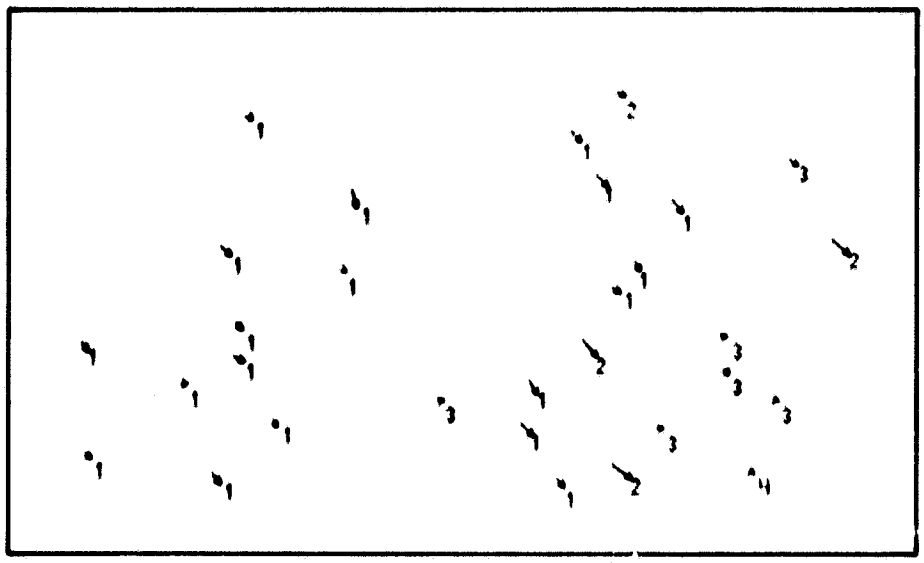

FIGURE 28 CLOUD MOTIONS COMPUTED USING VISIBLE TARGETS FOR THE THIRD PICTURE PAIR

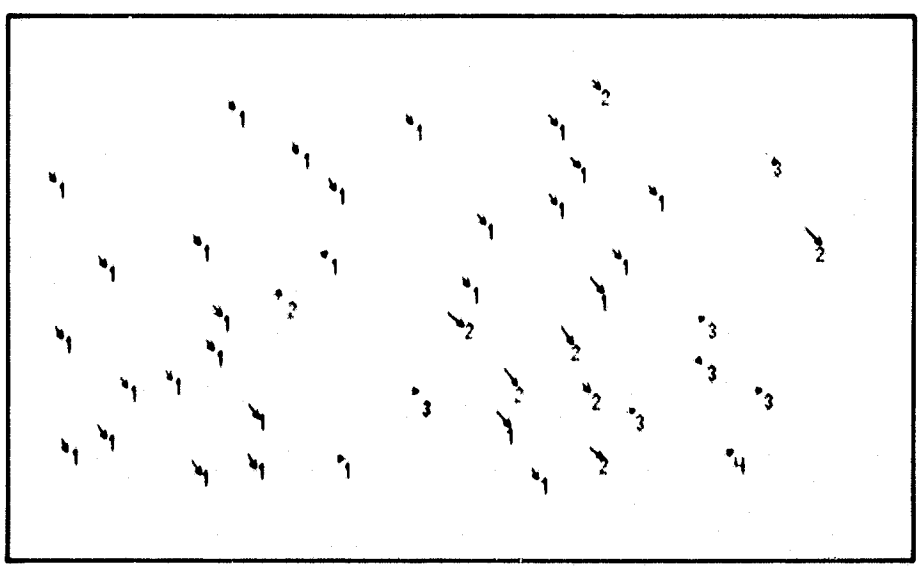

FIGURE 29 CLOUD MOTIONS COMPUTED BY CROSS CORRELATION FOR THE SAME GROUPS USED IN FIGURE 28

FIGURE 30 SEQUENCE OF MOTIONS OF VISIBLE TARGETS FOR FIVE PICTURE PAIRS, INCLUDING A 30-MINUTE INTERVAL

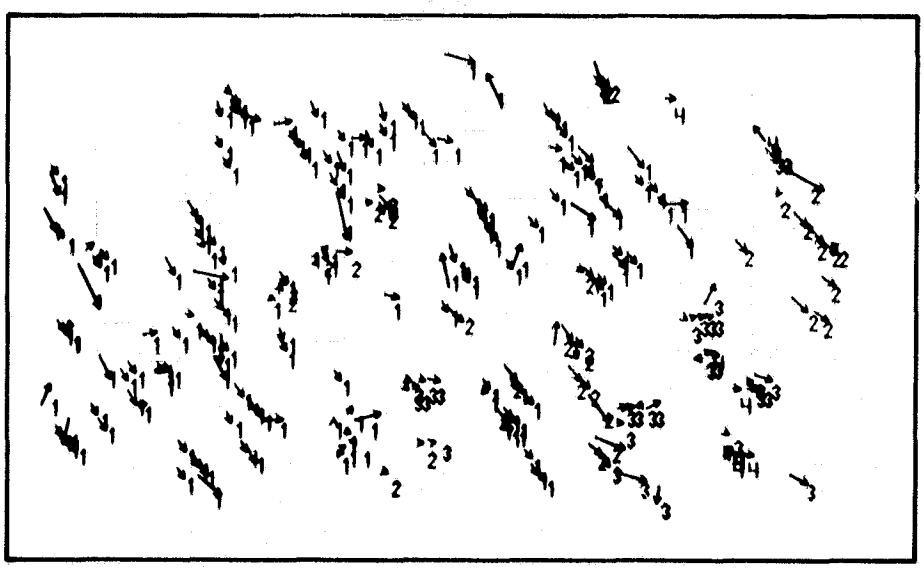

FIGURE 31 SEQUENCE OF MOTIONS FOR THE VISIBLE TARGETS OF FIGURE 30, COMPUTED BY CROSS CORRELATION

FIGURE 32 SEQUENCE OF MOTIONS FOR FIVE PICTURE PAIRS COMPUTED BY THE MOTION ROUTINE USING INFRARED DATA

To determine to what extent the results of the MOTION and COREL routines differ, we selected a set of targets with which to compare the computed cloud motions. We chose targets for which both methods had provided satisfactory results in terms of motion vectors that were in approximate agreement with other nearby vectors. Also, we selected only those targets for which the correlation coefficient was greater than 0.85. The data pertain to low clouds as shown in Figure 22 [Group (a)], middle and high clouds as shown in Figure 22 [Group (b)], and high clouds (including the edge of the cirrus sheet) shown in Figure 3 [Group (c)]. The results are given in Table 1. For Group (a), the average motion vectors for the MOTION and COREL routines differ by only 0.4 m s^{-1} in speed and 1 degree in direction, but the rms difference between individual vectors for the same targets is 6.7 m s^{-1} (0.5 pixels in ten minutes). For Group (b), the average motions differ by 2.0 m s^{-1} in speed and 6 degrees in directions, and the rms difference is 4.0 m s^{-1}. For Group (c), the average motions differ by 1.3 m s^{-1} in speed and 3 degrees in direction, and the rms difference is 11.4 m s^{-1}. It would be desirable to compare these computed vectors with visual tracking of the same targets; however, this was beyond the scope of our work. We believe that the level of agreement of the averages is satisfactory, and that the rms differences (which arise from differences in location of only fractions of a pixel) represent largely an unavoidable random component in computations of this sort.

Table 1

COMPARISON OF CLOUD MOTIONS (units m s^{-1})
COMPUTED USING THE MOTION AND CORRELATION ROUTINES

(a) Low Clouds, 25 Pairs, 4-km Visible Data (Figure 22)			
Average	Motion	Correlation	RMS Difference
u	15.5	15.8	3.9
v	-19.6	-18.8	5.4
Speed	24.9	24.5	6.7 (0.5 pixels)
Direction	321°	320°	
(b) High Clouds, 19 Pairs, 4-km Visible Data (Figure 22)			
Average	Motion	Correlation	RMS Difference
u	9.1	11.4	3.6
v	-3.8	-3.2	1.9
Speed	9.8	11.8	4.0 (0.3 pixels)
Direction	292°	286°	
(c) High Clouds, 42 Pairs, 4-km IR Data (from Figure 3)			
Average	Motion	Correlation	RMS Difference
u	-7.1	-8.4	8.8
v	30.4	28.7	7.1
Speed	31.2	29.9	11.4 (0.8 pixels)
Direction	167°	164°	

V SUMMARY AND CONCLUSIONS

In this research, the SRI automatic cloud tracking methods were substantially improved. Although the tests made are limited in number, the cases chosen for hurricane Eloise are very difficult ones even for human tracking; nevertheless, the automatic system performed very well. In simple cases there appears to be little doubt of the accuracy of the computed cloud motions, as we reported for the previous version of the methodology (Wolf et al., 1977). In complicated cases, some control over or editing of automatically computed motions may be needed.

The best results in terms of accuracy and coverage for the hurricane Eloise data were obtained using 4-km-resolution data at 10-minute intervals. For pictures separated by intervals of approximately 30 minutes, the automatic computations require data with coarser resolution in order to be able to track relatively high-speed motions. In other words, the method has the limitation that time and space scales must be matched so that the cloud displacements are less than 6 pixel units between pictures; if not, an approximate first guess of the displacement is needed so that the MOTION routine or the COREL routine will search in the right localities for matching groups. To a certain extent in such cases, SATS improves its first guess from the first one or two picture pairs of a sequence, so that tracking is reliable in later pairs. Alternatively, computations made with coarse-resolution data can be used as a first guess for more detailed and accurate computations with finer resolution data.

An important new option has been added to the methodology in terms of the cross-correlation computation of motions. In this option the targets are selected automatically, but the displacements are computed by a search routine that locates the point of highest correlation--i.e., the COREL routine replaces the MOTION routine. Both routines give satisfactory results. For typical targets the displacements computed by the MOTION and COREL routines differ by only fractions of a pixel. In our opinion this level of accuracy is as high as one can expect since the data contain small-scale time-varying features.

At this time we believe that more extensive tests should be made by including SATS in an interactive system such as AOIPS, where it can be applied to a large number of cases. The results can then be checked directly against measurements made under operator control. Experienced analysts should then be able to make a comprehensive comparison and evaluation of the different options and methods.

REFERENCES

Bauer, K. G., 1976: A comparison of cloud motion winds with coinciding radiosonde winds. Mon. Wea. Rev., 104, 922-931.

Billingsley, J. B., 1976: Interactive image processing for meteorological applications at NASA/Goddard Space Flight Center. Preprints, Seventh Conf. Aerospace and Aeronautical Meteorology, Melbourne, Amer. Meteor. Soc., 268-275.

Endlich, R. M., D. E. Wolf, D. J. Hall, and A. E. Brain, 1971: Use of a pattern recognition technique for determining cloud motions from sequences of satellite photographs. J. Appl. Meteor., 10, 104-117.

Hall, D. J., R. M. Endlich, D. E. Wolf, and A. E. Brain, 1972: Objective methods for registering landmarks and determining cloud motions from satellite data. IEEE Trans. Comput., C-21, 768-776.

Hasler, A. F., W. Shenk, and J. P. Gary, 1976: A study of a STORMSAT interactive data analysis facility. Preprints, Seventh Conf. Aerospace and Aeronautical Meteorology, Melbourne, Amer. Meteor. Soc., 284-290.

Leese, J. A., C. S. Novak, and B. B. Clark, 1971: An automated technique for obtaining cloud motion from geosynchronous satellite data using cross correlation. J. Appl. Meteor., 10, 118-132.

Rodgers, E., R. C. Gentry, W. Shenk, and V. Oliver, 1979: The benefits of using short-interval satellite images to derive winds for tropical cyclones. Mon. Wea. Rev., 107, 575-584.

Serebreny, S. M., E. J. Weigman, R. G. Hadfield, and W. E. Evans, 1970: Electronic system for utilization of satellite cloud pictures. Bull. Amer. Meteor. Soc., 51, 848-855.

Smith, E., 1975: Man-computer interactive data access system. IEEE Trans. Geosci. Electron., GE-13, 123-126.

Wolf, D. E., R. M. Endlich, and D. J. Hall, 1977: Experiments in automatic cloud tracking using SMS-GOES data. J. Appl. Meteor., 16, 1219-1230.